American Journal of Pathology, Vol. 162, No. 3, March 2003

AIM Inhibits Apoptosis of T Cells and NKT Cells in *Corynebacterium*-Induced Granuloma Formation in Mice

Kazuhisa Kuwata,* Hisami Watanabe,† Shu-Ying Jiang,* Takashi Yamamoto,* Chikako Tomiyama-Miyaji,‡§ Toru Abo,‡ Toru Miyazaki,¶ and Makoto Naito*

From the Department of Cellular Function, Division of Cellular and Molecular Pathology and the Division of Immunology and Medical Zoology,‡ Niigata University Graduate School of Medical and Dental Sciences, Niigata, Japan; the Department of Medical Technology,§ School of Health Sciences, Faculty of Medicine, Niigata University, Niigata, Japan; the Division of Cellular and Molecular Immunology, Center of Molecular Biosciences,† University of the Ryukyus, Nishihara, Okinawa, Japan; and the Center for Immunology,¶ The University of Texas Southwestern Medical Center, Dallas, Texas*

Apoptosis inhibitor expressed by macrophages (AIM) inhibits apoptosis of $CD4^+CD8^+$ (CD4/CD8) double-positive thymocytes, and supports the viability of these cells on the thymic selection. However, pleiotropic functions of AIM have been suggested. In this study, heat-killed *Corynebacterium parvum* (*C. parvum*) was injected into mice carrying the homozygous mutation ($AIM^{-/-}$) and wild-type ($AIM^{+/+}$) mice, to investigate the role of AIM in the formation of hepatic granulomas. In $AIM^{-/-}$ mice, the size and the number of hepatic granulomas were larger, and the resorption of granulomas was more delayed than in $AIM^{+/+}$ mice. The production of interleukin-12 was more prominent in $AIM^{-/-}$ mice than in $AIM^{+/+}$ mice. In the liver of $AIM^{+/+}$ mice, expression of AIM messenger ribonucleic acid (mRNA) increased after *C. parvum* injection. *In situ* hybridization demonstrated that AIM mRNA was expressed in Kupffer cells and exudate macrophages in the liver, especially in granulomas. Larger numbers of T cells and natural killer T (NKT) cells underwent apoptosis in the granulomas of $AIM^{-/-}$ mice, suggesting that AIM prevents apoptosis of NKT cells and T cells in *C. parvum*-induced inflammation. Recombinant AIM (rAIM) protein significantly inhibited apoptosis of NKT cells and T cells obtained from *C. parvum*-stimulated livers *in vitro*. These results indicate that AIM functions to induce resistance to apoptosis within NKT cells and T cells, and supports the host defense in granulomatous inflammation. ***(Am J Pathol 2003, 162:837–847)***

Apoptosis inhibitor expressed by macrophages (AIM) is a murine macrophage-specific 54-kd secreted protein, and belongs to the macrophage scavenger receptor cysteine-rich domain superfamily (SRCR-SF).[1] Thymic small lymphocytes, commonly known as thymocytes, are highly radiosensitive. Notably, immature thymocytes such as $CD4^+CD8^+$ (CD4/CD8) double-positive T cells easily undergo apoptosis within a few hours after irradiation[2–4] and the administration of glucocorticoid.[5–9] The CD4/CD8 double-positive thymocytes in AIM-deficient mice ($AIM^{-/-}$) were strikingly more susceptible to apoptosis by irradiation and dexamethasone *in vivo*. Recombinant AIM (rAIM) protein inhibited cell death of these cells in response to a variety of stimuli *in vitro*. Thus, AIM functions in the thymus as the inducer of resistance to apoptosis within CD4/CD8 double-positive thymocytes, and as the supporter of the viability of these cells before thymic selection.[1] AIM also induces growth inhibition of B lymphocytes.[10] Recently, it was also demonstrated that AIM supports macrophage survival and enhances phagocytic function of macrophages in *Corynebacterium parvum* (*C. parvum*)-induced hepatitis.[11] Thus AIM has been suggested to exhibit different functions to various types of target cells.

Granuloma formation is a kind of inflammatory process accompanied by focal accumulation of inflammatory cells and production of several cytokines.[12–13] Macrophages, lymphocytes, and other inflammatory cells play a central role in granulomatous inflammation through humoral and cell-cell interaction mechanisms. Apoptosis of inflammatory cells as well as tissue cells also plays a pivotal role in inflammation.[14–22] Both positive and negative regulation of apoptosis of cells influence the initiation, progression, or healing of tissue damage and the balance of these two regulations may critically influence the inflammatory process. Fas-Fas ligand and TNF-α-mediated mechanisms are involved in the inflammatory tissue damage. We have shown that AIM was expressed in a subset of macrophages in bacillus Calmette Guérin (BCG)-induced hepatic granulomas.[1] Although extracel-

Supported by Grants-in-Aid for Scientific Research from the Ministry of Education, Science, and Culture of Japan.

Accepted for publication November 21, 2002.

Address reprint requests to Makoto Naito, M.D., Department of Cellular Function, Division of Cellular and Molecular Pathology, Niigata University Graduate School of Medical and Dental Sciences, Asahimachi-dori 1, Niigata 951-8510 Japan. E-mail: mnaito@med.niigata-u.ac.jp.

lular apoptosis inhibitory elements have not been well defined so far, AIM appears to mediate inhibitory signals for apoptosis of some inflammatory cells and modulate the inflammatory process.

In this report, we have applied a mouse model to address potential involvement of AIM in the process of granulomatous inflammation *in vivo*. In addition, we present a novel function of AIM associated with apoptosis inhibitory effect on natural killer T (NKT) cells and T lymphocytes.

Materials and Methods

Animals

Mice deficient in AIM were generated by disruption of exon 3 of the AIM gene, which encodes the second scavenger receptor cysteine-rich domain (SRCR domain) of AIM.[1] E-14.1 embryonic stem (ES) cells containing the disrupted AIM gene by pMC1-neo-polyA (Stratagene, La Jolla, CA) plasmid, were isolated as G418-resistant, screened by polymerase chain reaction (PCR) and Southern blotting, were injected into C57Bl/6 (B6) (Charles River Japan, Inc., Yokohama, Japan) blastocysts, and chimeric male offspring were mated to B6 females. Mice carrying the mutation in the heterozygous state ($AIM^{+/-}$) were intercrossed to produce homozygous mutants ($AIM^{-/-}$). Eight-to-12-week-old $AIM^{-/-}$ mice and wild-type ($AIM^{+/+}$) B6 mice were used for analysis.

Heat-killed *C. parvum* (*Propionibacterium acnes*; *P. acnes)* (The Van Kampen Group, Inc., North Chicago, IL), 0.5 mg, was injected into the tail vein. All mice were killed under diethyl ether anesthesia at 1, 3, 5, 7, 10, 14, 17, 21, and 28 days after injection, and their livers, spleens, kidneys, lungs, hearts, and appendixes were removed. Body and liver weights were measured for each mouse. A part of each liver was frozen in liquid nitrogen and stored for messenger ribonucleic acid (mRNA) analysis; the others were fixed for morphological studies.

Histology and Evaluation of Hepatic Granulomas

Tissue was fixed in 10% formaldehyde and embedded in paraffin. Paraffin sections were stained with hematoxylin and eosin for light microscopy. Hepatic granulomas were defined as being composed of more than 10 white blood cells.[23–25] The number of granulomas per 1-mm^2 section was counted. In each section, 50 granulomas were randomly selected, and then their mean diameters were measured. Based on the mean diameter, the mean area size of the granulomas was calculated. Neutrophils were stained by the naphthol AS-D chloroacetate esterase method.[26] The number of gram-positive rods in macrophages was counted in the liver at 1 day after *C. parvum* injection.

Immunohistochemistry

Liver tissues were fixed in 2% periodate-lysine-paraformaldehyde (PLP) solution at 4°C for 4 hours, washed for 6 hours with phosphate buffer solution containing 10%, 15%, and 20% sucrose, finally washed for 30 minutes with phosphate buffer solution (PBS) containing 20% sucrose and 5% glycerin, embedded in OCT compound (Sakura, Tokyo, Japan), frozen at −80°C, and cut by a cryostat (Bright, Huntington, UK) into 6-μm-thick sections. After inhibition of endogenous peroxidase activity by the method of Isobe et al,[27] we performed immunohistochemistry using the anti-mouse macrophage monoclonal antibody F4/80[28] (BMA Biomedicals, August, Switzerland), anti-mouse T lymphocyte monoclonal antibody Thy1.2, anti-mouse B lymphocyte monoclonal antibody B220 (Becton Dickinson, Mountain View, CA). As secondary antibody, we used anti-rat Ig-horseradish peroxidase-linked $(ab')^2$ fragment (Amersham, Poole, UK) to F4/80, Thy1.2, and B220. After visualization with 3,3′-diaminobenzidene (Dojin Chemical Co., Kumamoto, Japan), the sections were stained with methylene green for nuclear staining and mounted with resin.

Enzyme-Linked Immunosorbent Assay for the Detection of Interferon-γ, Interleukin-4, Interleukin-10, and Interleukin-12

Sera obtained from each mouse were used to detect the concentrations of interferon-γ (IFN-γ), interleukin-4 (IL-4), interleukin-10 (IL-10) and interleukin-12 (IL-12) by enzyme-linked immunosorbent assay (ELISA) using the Opt EIA mouse IFN-γ and IL-4 sets (Pharmingen, San Diego, CA) and the ENDOGEN Mouse Interleukin-10 and Interleukin-12 Total ELISA kits (Endogen, Woburn, MA).

Reverse Transcriptase-Polymerase Chain Reaction

Total cellular ribonucleic acid (RNA) was isolated from liver tissues by the acid guanidium thiocyanate-phenol-chloroform method. Two micrograms of total RNA was converted to complementary DNA (cDNA) by reverse transcription using a SuperScript Preamplification kit (Gibco BRL, Gaithersburg, MD) with the oligo(dt) primer. PCR amplification of synthesized cDNA was conducted using 2 μl of each cDNA added to a reaction mixture containing 5 μl of PCR amplification buffer, 2 μl of 25 mmol/L $MgCl_2$, 4 μl of 2.5 mmol/L deoxyribonucleotide 3-phosphates mix (dNTPs mix), 2 μl of 20 mmol/L each primer, 0.3 μl of 5 units/μl *Taq* polymerase (Promega, Madison, WI), and 32.7 μl double-distilled water in a reaction volume of 50 μl. The primers used in this study are shown in Table 1. Thirty-five cycles consisted of 1 minute at 94°C, 2 minutes at 55°C, and 2 minutes at 72°C. These PCR amplifications were performed with using a Program Temp Control system PC-700 (ASTEC, Tokyo, Japan). A 10-μl production of each amplified product was examined by 2% agarose gel electrophoresis containing 0.5 μg/ml ethidium bromide. Bands were visualized and photographed by ultraviolet transillumination.

In Situ *Hybridization*

Mice were perfused through the heart with 4% paraformaldehyde and, after removal, the liver was refixed in the

Table 1. Sequences of Oligonucleotide Primers Used for RT-PCR

mRNA	Primers (5′–3′)	Sequences (5′ to 3′)	Products (bp)
AIM	Sense	TTG GAG AAC AAC TGT ACC CAT GGC	468
	Anti-sense	AGG CTG AGG GAA AGG TGT CTA AAG	
IL-1β	Sense	CTC TAG AGC ACC ATG CTA CAG AC	309
	Anti-sense	TGG AAT CCA GGG GAA ACA CTG	
IL-4	Sense	CGA AGA ACA CCA CAG AGA GTG AGC T	180
	Anti-sense	GAC TCA TTC ATG GTG CAG CTT ATC G	
IL-6	Sense	TGG AGT CAC AGA AGG AGT GGC TAA G	166
	Anti-sense	TCT GAC CAC AGT GAG GAA TGT CCA C	
IL-10	Sense	TAC CTG GTA GAA GTG ATG CC	255
	Anti-sense	CAT CAT GTA TGC TTC TAT GC	
IL-12	Sense	CGT GCT CAT GGC TGG TGC AAA G	314
	Anti-sense	CTT CAT CTG CAA GTT CTT GGG C	
IFN-γ	Sense	AGC GGC TGA CTG ACC TCA GAT TGT AC	213
	Anti-sense	GTC ACA GTT TTC AGC TGT ATA GGG	
TNF-α	Sense	GGC AGG TCT ACT TTG GAG TCA TTG C	309
	Anti-sense	ACA TTC GAG GCT CCA GTG AAT TCG G	
MIP-2	Sense	CAA AGG CAA GGC TAA CTG	532
	Anti-sense	TGT TCT ACT CTC CTC GGT	
MCP-1	Sense	CTC ACC TGC TGC TAC TCA TTC	350
	Anti-sense	GCA TGA GCT GGT TGT GAA AAA	
MCP-3	Sense	GTG CCT GAA CAG AAA CCA ACC T	150
	Anti-sense	CAT TCC TTA GGC GTG ACC ATT	
M-CSF	Sense	ACT GTA GCC ACA TGA TTC G	410
	Anti-sense	GCT GTT GTT GCA GTT CTT G	
β-actin	Sense	TGG AAT CCT GTG GCA TGC ATG AAA C	348
	Anti-sense	TAA AAC GCA GCT CAG TAA CAG TCC G	

same fixative for 24 hours. Tissues were dehydrated in ethanol, cleared in chloroform, and embedded in low-melting-point paraffin (Tissue Prep, No. T565, melting point 56 to 57°C, Fisher Scientific, Fair Lawn, NJ). Sections were cut and mounted onto 3-aminopropyl-triethoxysilane- (Aldrich Chemical Co., Milwaukee, WI) coated slides. Paraffin sections of the liver were subjected to *in situ* hybridization by using digoxigenin-labeled (Boehringer-Mannheim, Mannheim, Germany) hybridizing (antisense) and non-hybridizing (sense) RNA probes transcribed from AIM cDNA subcloned in pBluescript streptokinase (SK)(+) (Stratagene) plasmid by T3 or T7 RNA polymerases. Sections were then treated with anti-digoxigenin-alkaline phosphatase, and developed by 4-nitroblue tetrazolium chloride.

Terminal Deoxynucleotidyl Transferase-Mediated Deoxyribonucleoside Uridine Triphosphate-Biotin Nick End Labeling Assay

The terminal deoxynucleotidyl transferase (TdT)-mediated deoxyribonucleoside uridine triphosphate (dUTP)-biotin nick end labeling (TUNEL) method, which based on the specific binding of TdT to the 3′-OH ends of DNA, was performed for detection of cells undergoing apoptosis.[29] To inactivate endogenous peroxidase, each PLP-fixed section was covered with 2% H_2O_2 for 5 minutes at room temperature as well as immunohistochemistry. Then, the sections were rinsed and immersed in TdT buffer (30mmol/L Trizma base, pH 7.2, 140 mmol/L potassium cacodylate, 1 mmol/L $CaCl_2$) containing biotinylated dUTP, introduced by TdT, and stained with avidin-conjugated peroxidase. The negative controls were stained by omitting TdT from the TdT buffer to ensure that endogenous peroxidase was adequately inactivated. For nuclear staining, the sections were stained with methylene green after visualization with 3,3′-diaminobenzidene (Dojin).

Cell Preparations and Cell Cultures

Mice were sacrificed by exsanguination from the subclavian artery and vein, and then the liver was removed. Hepatic mononuclear cells (MNC) were prepared as previously described.[30] Briefly, the liver was pressed through stainless steel mesh and suspended in Eagle's minimum essential medium (MEM) supplemented with 5 mmol/L HEPES and 2% fetal calf serum (FCS). After washing once, the cells were resuspended in 35% Percoll solution containing 100 units/ml heparin and centrifuged at 2000 rpm for 15 minutes. The cell pellet resuspended in red blood cell lysis solution (155 mmol/L NH_4Cl, 10 mmol/L $KHCO_3$, 1 mmol/L EDTA, 170 mmol/L Tris, pH 7.3) and then washed twice with medium. For analyzing the surface phenotype of cultured cells, MNC (1×10^7 cells per well) were cultured in 24-well microculture plates with or without rAIM protein for 24 hours.

Flow Cytometric Analysis and Detection of Cells Undergoing Apoptosis

The surface phenotype of cells was analyzed using monoclonal antibodies (mAbs) in conjunction with a two- or three-color immunofluorescence test.[30] Fluorescein isothiocyanate (FITC)-, phycoerythrin (PE)-, or biotin-conjugated anti-CD3 (145–2C11) and anti-NK1.1 (PK136) mAbs were obtained from PharMingen. Biotin-conjugated reagents were developed with tricolor-conjugated

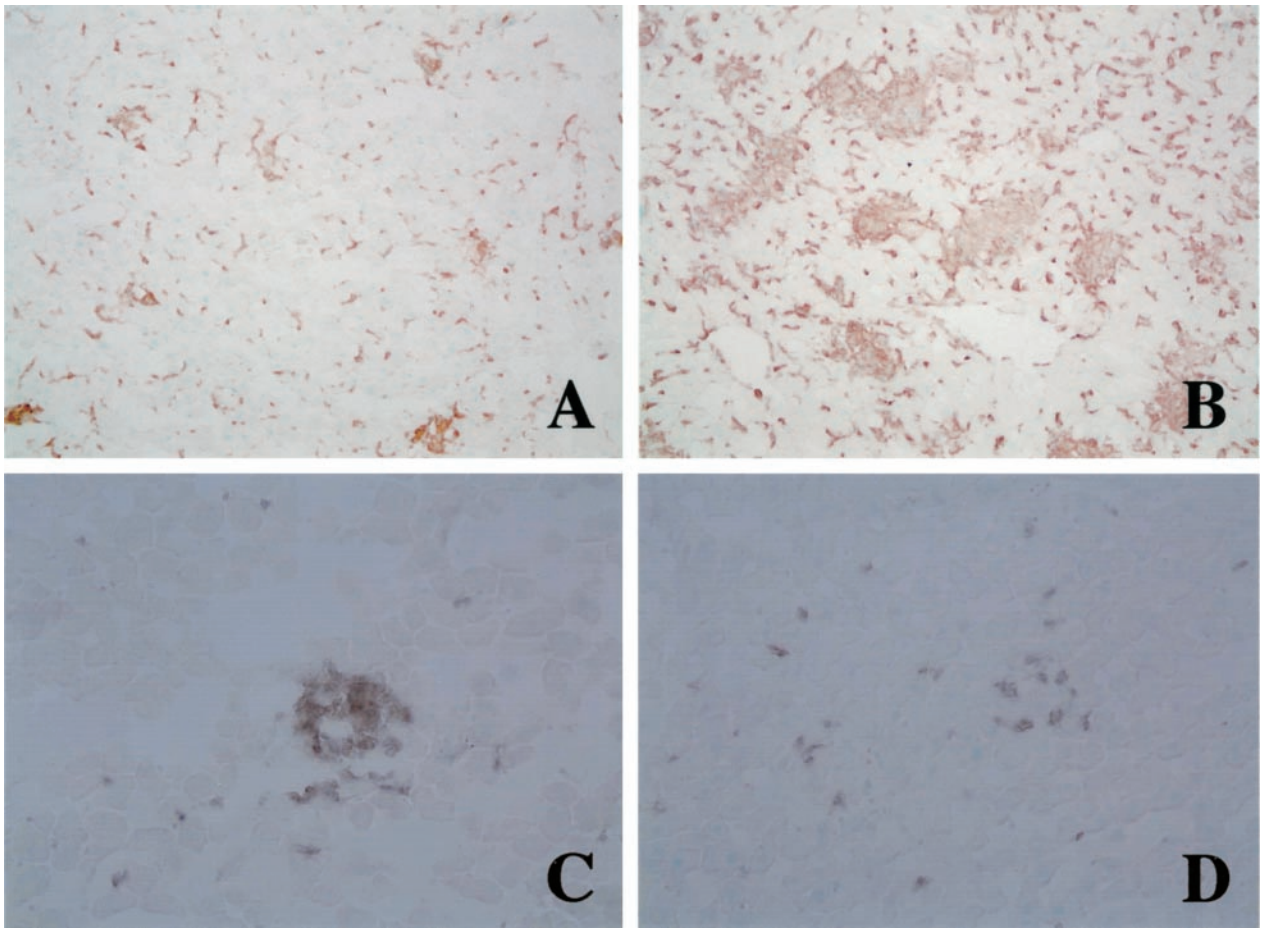

Figure 1. Immunohistochemistry of *C. parvum*-injected livers of homozygous mutant ($AIM^{-/-}$) (**B** and **D**) and wild-type ($AIM^{+/+}$) mice (**A** and **C**) at 17 days after injection. **A** and **B:** Accumulations of $F4/80^{+}$ macrophages and granuloma formation are more prominent in an $AIM^{-/-}$ mouse (**B**) than in an $AIM^{+/+}$ mouse (**A**). Original magnification, ×100. **C** and **D:** Infiltration of $Thy1.2^{+}$ T cells in the granulomas of an $AIM^{-/-}$ mouse (**D**) is less remarkable than that of an $AIM^{+/+}$ mouse (**C**). Original magnification, ×200.

streptavidin (Calrag Laboratories, San Francisco, CA). To prevent non-specific binding of mAbs, CD32/16 (2.4G2) (Pharmingen) was added before staining with labeled mAbs. The fluorescence-positive cells were analyzed by FACScan (Becton Dickinson). Dead cells were excluded by forward scatter, side scatter, and propidium iodide (PI) gating. To determine the percentage of cells undergoing apoptosis, FITC-labeled Annexin V (Pharmingen) was used following the manufacturer's instructions.[31] Isolated cells and cultured cells were stained with those anti-CD3 and anti-NK1.1 mAbs. After washing with PBS (pH 7.4) twice, these cells were stained with FITC-conjugated Annexin V and analyzed by flow cytometry.

AIM Transfectants and Recombinant AIM

AIM cDNA was subcloned into an expression vector, which contains cytomegarovirus enhancer, chicken β-actin promoter, and rabbit β-globin exons and intron. The resulting construct (pAc-AIM) was contransfected with pMC1-neo-polyA (Stratagene) into Chinese hamster ovary (CHO) cells by electroporation. Three resistant clones, which were selected by G148 and detected high amounts of AIM protein production by Western blot analysis using an anti-AIM antibody, were obtained. One of them was used as an AIM transfectant. Conditioned medium from this transfectant, as well as from non-transfected CHO cells as a control, was used for *in vitro* functional analysis of AIM. Approximate concentration of rAIM in the conditioned medium from transfectants was evaluated by Western blotting using titrated purified rAIM generated by *Trichoplusia ni* egg cells as controls.[1]

Statistical Examination

Values were expressed as means ± standard deviation (SD). Then each mean values of each group were compared by the use of Mann-Whitney-*U*-test. The mean numbers of *C. parvum* per macrophage were statistically evaluated by unpaired Student's *t*-test.

Results

Granuloma Formation in the Liver of $AIM^{-/-}$ and $AIM^{+/+}$ Mice

In untreated $AIM^{+/+}$ mice, Kupffer cells were specifically immunostained with F4/80. Three days after *C. parvum* in-

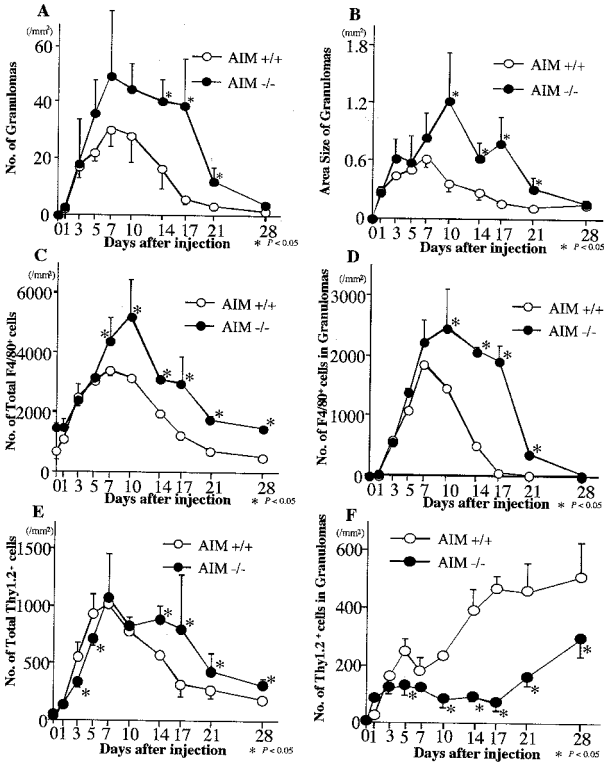

Figure 2. The number (**A**) and area size (**B**) of granulomas in livers, the numbers of macrophages in the liver (**C**) and in the granulomas (**D**), and the numbers of Thy 1.2^+ T cells in the liver (**E**) and in the granulomas (**F**) of $AIM^{-/-}$ and $AIM^{+/+}$ mice after *C. parvum* injection. **A** and **B:** $AIM^{-/-}$ mice develop larger numbers of granulomas than $AIM^{+/+}$ mice. **C** and **D:** Larger numbers of macrophages were present in the liver and granulomas in $AIM^{-/-}$ mice than $AIM^{+/+}$ mice. **E** and **F:** The numbers of T cells had not remarkable difference in the liver, but there were smaller numbers of T cells in the granulomas of $AIM^{-/-}$ than in $AIM^{+/+}$ mice. Data are shown as the mean ± SD of five mice. *, $P < 0.05$.

jection, a few clusters of neutrophils, macrophages, and lymphocytes were found in the liver of $AIM^{+/+}$ mice. Granuloma formation followed (Figure 1A). The number of granulomas increased until 7 days, gradually decreased, and was mostly diminished at 21 days (Figure 2A). The area size of granulomas was largest at day 7 (Figure 2B). The number of F4/80-positive ($F4/80^+$) cells in the liver and in the granulomas increased until 7 days after injection (Figure 2, C and D). In the granulomas, $F4/80^+$ cells occupied about 30% of the granuloma-constituting cells at 3 days and were doubled at 7 days. Each size of the macrophages became larger, and macropahges transformed into epithelioid cells and multinuclear giant cells after 7 days, but had mostly diminished at 17 days (Figure 1A and Figure 2, C and D). Most of infiltrated lymphocytes were Thy-1.2-positive ($Thy1.2^+$) cells. $Thy1.2^+$ T lymphocytes were detectable in and around the granulomas (Figure 1C). They were mainly situated at the periphery of the granulomas. The number of $Thy1.2^+$ cells in the liver increased by 7 days (Figure 2E) and $Thy1.2^+$ cells occupied about 18% of the granuloma-constituting cells. Only a few B220-positive ($B220^+$) B lymphocytes were present in the granulomas all through the series.

In $AIM^{-/-}$ mice, the number of granulomas was largest also at 7 days (Figure 2A). Granulomas often fused to each other after 7 days in the liver of $AIM^{-/-}$ mice (Figure

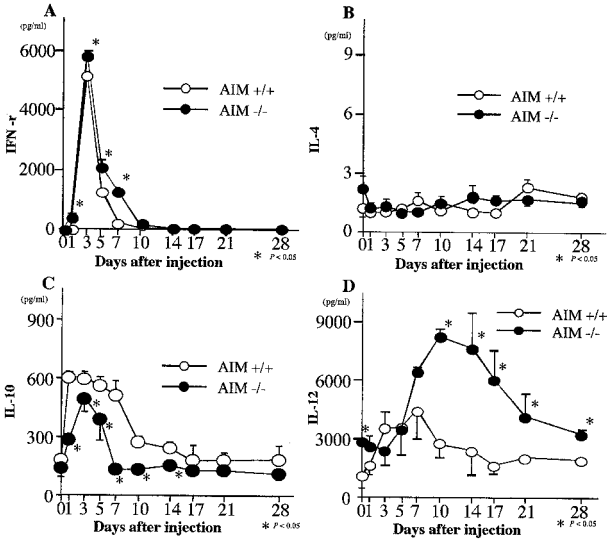

Figure 3. Serum concentrations of IFN-γ (**A**), IL-4 (**B**), IL-10 (**C**), and IL-12 (**D**) in $AIM^{-/-}$ and $AIM^{+/+}$ mice after *C. parvum* injection. Serum levels of IL-12 and IFN-γ were higher in $AIM^{-/-}$ than in $AIM^{+/+}$ mice. Serum levels of IL-10 were lower in $AIM^{-/-}$ than $AIM^{+/+}$ mice. Data are shown as the mean ± SD of three mice. *, $P < 0.05$.

1B). The number and the area size of granulomas in $AIM^{-/-}$ mice were larger than those in $AIM^{+/+}$ mice (Figure 2, A and B). The numbers of macrophages in the granulomas of the $AIM^{-/-}$ mice became larger than those of $AIM^{+/+}$ mice after day 7 (Figure 1, A and B, and Figure 2, C and D). On the numbers of T cells in the liver, there were not any remarkable differences between $AIM^{-/-}$ and $AIM^{+/+}$ mice until day 10 (Figure 2E). But the numbers of T lymphocytes in the granulomas were smaller in the $AIM^{-/-}$ mice than those in the $AIM^{+/+}$ mice after day 3 (Figure 1, C and D, and Figure 2F).

As for the numbers of *C. parvum* in macrophages at 1 day after injection, the average number of phagocytized bacilli in macrophage of $AIM^{+/+}$ mice was 12.2 ± 3.8, while that of $AIM^{-/-}$ mice was 8.8 ± 2.8, $P = 0.0013$), indicating that phagocytic capacity of macrophages was deficient in $AIM^{-/-}$ mice.

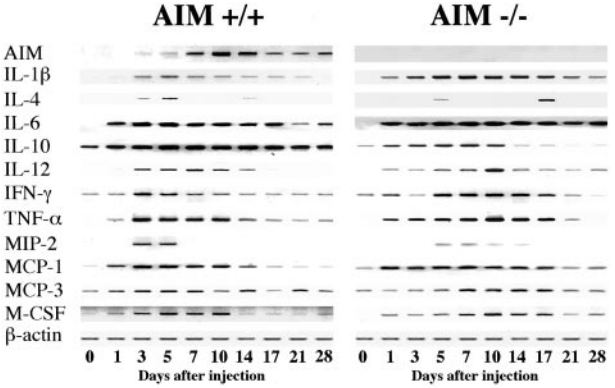

Figure 4. Expression of AIM, cytokines, and β-actine mRNAs of $AIM^{-/-}$ and $AIM^{+/+}$ mice after *C. parvum* injection. The result from one of three similar experiments is shown.

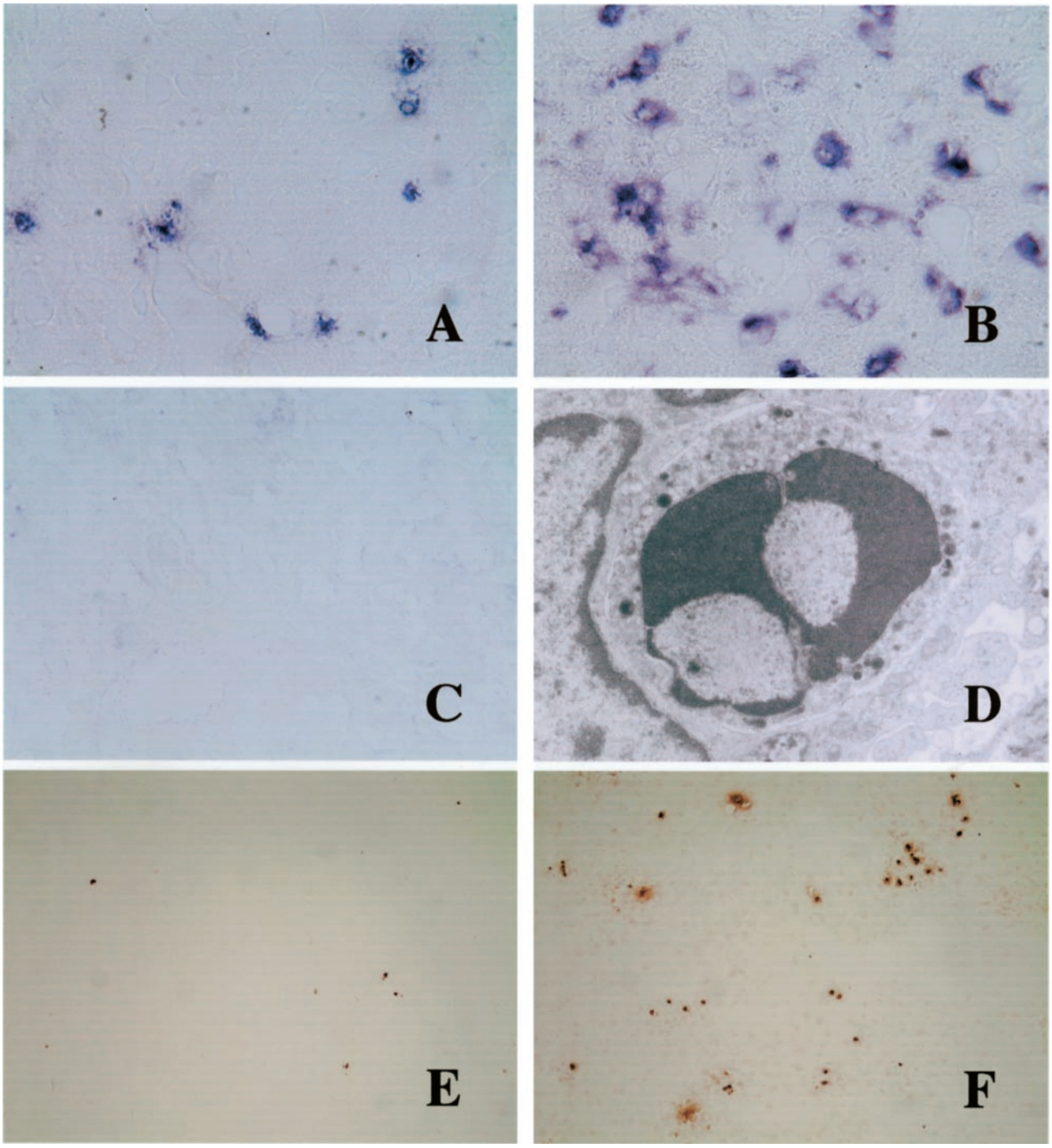

Figure 5. AIM mRNA expression in the liver by *in situ* hybridization (**A-C**), electron micrograph of an apoptotic lymphocyte (**D**), and TUNEL-staining of apoptotic cells (**E** and **F**). **A–C:** AIM mRNA is weakly expressed in a few round or spindle cells along the hepatic sinusoids of untreated $AIM^{+/+}$ mice (**A**). At day 17 after *C. parvum* injection, AIM expression is augmented in macrophages (**B**), especially in granulomas. However, signal-positive cells were not detected in the liver of *C. parvum*-injected and non-injected $AIM^{-/-}$ mice (**C**). Original magnification, ×400. **D:** Electron micrograph of a lymphocyte in the granuloma with small electron-dense intracytoplasmic granules. Condensed nucleus suggests apoptosis of this granular lymphocyte. Original magnification, ×12,000. **E** and **F:** At 17 days TUNEL-labeled cells are more abundant in the liver of $AIM^{-/-}$ mice (**F**) than in $AIM^{+/+}$ mice (**E**). Original magnification, ×40.

Serum Cytokine Levels of $AIM^{-/-}$ and $AIM^{+/+}$ Mice

The serum levels of IFN-γ and IL-12 were higher in $AIM^{-/-}$ mice than in $AIM^{+/+}$ mice (Figure 3, A and D). The serum concentrations of IL-10 were lower in $AIM^{-/-}$ mice than in $AIM^{+/+}$ mice, especially from day 1 to 14, there were significant differences between both groups (Figure 3C). However, the level of serum IL-4 was not remarkably different between both mice (Figure 3B).

Expression of Cytokine Messenger Ribonucleic Acids in the Liver of AIM$^{-/-}$ and AIM$^{+/+}$ Mice

Expressions of interleukin-1β (IL-1β), IL-4, interleukin-6 (IL-6), IL-10, IL-12, IFN-γ, tumor necrosis factor-α (TNF-α), macrophage inflammatory protein-2 (MIP-2), monocyte chemoattractant protein-1 (MCP-1), monocyte chemoattractant protein-3 (MCP-3), and macrophage colony-stimulating factor (M-CSF) mRNA were enhanced in both mice after *C. parvum* injection. Most of the cytokine mRNA expression patterns were similar between both mice. Comparing the groups, IL-10 mRNA expression was less remarkable in the liver of AIM$^{-/-}$ mice. On the other hand, IL-12 and MCP-1 mRNA expressions were enhanced in the liver of AIM$^{-/-}$ mice (Figure 4).

Expression of AIM and In Situ *Expression of AIM mRNAs in the Liver of AIM$^{-/-}$ and AIM$^{+/+}$ Mice*

Reverse transcriptase-polymerase chain reaction (RT-PCR) analysis demonstrated that expression of AIM mRNA was not detected in the livers of non-treated AIM$^{+/+}$ mice and AIM$^{-/-}$ mice. At 3 days after injection, AIM expression in the livers of AIM$^{+/+}$ mice was enhanced and reached a maximum level at day 10, and was followed by gradual decreases (Figure 4).

In situ hybridization revealed that there are a few AIM mRNA expressing cells along the hepatic sinusoids in the untreated AIM$^{+/+}$ mice (Figure 5A). Three days after *C. parvum* injection, a larger number of cells in the sinusoid showed the positive signals of AIM mRNA. The number of AIM expressing cells at 10 days was largest and these positive cells decreased unsubstantially (Figure 5B). These cells were mononuclear, round or spindle in shape, and scattered in the sinusoid and in the peripheral area of granulomas. No expression of AIM mRNA was confirmed in endothelial cells or hepatocytes. In AIM$^{-/-}$ mice, AIM mRNA was not expressed in any cells in the liver throughout the experimental period (Figure 5C).

Detection of Apoptosis in C. parvum*-Induced Granulomatous Inflammation*

The number of apoptotic cells as detected by TUNEL method increased after *C. parvum* injection in both mice. The number of apoptotic cells in the liver of AIM$^{+/+}$ mice increased until day 3, then was followed by gradual decreases (Figure 6). However, the numbers of apoptotic cells in AIM$^{-/-}$ mice increased up to day 14 and were significantly larger than those in AIM$^{+/+}$ mice after day 14 (Figure 5, E and F, and Figure 6). Electron microscopically apoptosis of several inflammatory cells were observed. Lymphocytes including granular lymphocytes also underwent apoptosis (Figure 5D).

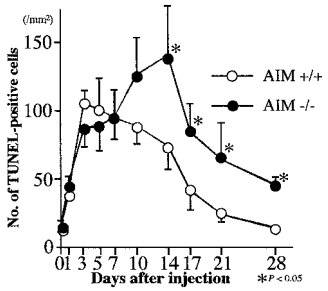

Figure 6. The numbers of TUNEL-labeled cells in the liver of AIM$^{-/-}$ and AIM$^{+/+}$ mice after *C. parvum* injection. After 7 days, larger numbers of apoptotic cells were present in the liver of AIM$^{-/-}$ mice than AIM$^{+/+}$ mice. Data are shown as the mean ± SD of three mice. *, $P < 0.05$.

NKT and T Cell Disappearance and Apoptosis Detected by Flow Cytometric Analysis

In untreated conditions, the proportion of CD3$^+$NK1.1$^+$ NKT cells in the liver was slightly smaller in AIM$^{-/-}$ mice than in AIM$^{+/+}$ type mice (Figure 7A). In contrast, the proportion of CD3$^+$NK1.1$^-$ conventional T cells in the AIM$^{-/-}$ mice was slightly larger than that in AIM$^{+/+}$ mice (Figure 7A). But, as for the absolute numbers of these cells, there were no significant differences between both groups (Figure 8). There were numerical increases of conventional T cells after *C. parvum* injection in the liver of both types of mice, peaking at day 7 (Figure 8A). The numbers of natural killer (NK) and NKT cells also increased in both types of mice (Figure 8, B and C). After day 7 the numbers of NKT cells in AIM$^{+/+}$ mice remained at high levels, but there was a rapid decrease of those in AIM$^{-/-}$ mice (Figure 8C).

We then examined the apoptosis of NKT cells and conventional T cells by flow cytometry using Annexin V. The binding of Annexin V to both types of cells, especially NKT cells, was more abundant in AIM$^{-/-}$ mice than in AIM$^{+/+}$ mice at day 1, 3, and 17. It indicated to us that larger numbers of NKT cells and conventional T cells in the liver of the AIM$^{-/-}$ mice underwent apoptosis than in AIM$^{+/+}$ mice (Figure 7B).

We next evaluated the inhibition effect of rAIM protein in *in vitro* culture systems. The liver MNCs obtained from *C. parvum* injected AIM$^{-/-}$ mice were cultured with or without rAIM protein for 24 hours. The cells cultured with rAIM protein were more diminished in the numbers and mean fluorescence intensities of Annexin V-positive apoptotic cells, especially in NKT cells and conventional T cells, than those without rAIM protein. In the fraction of NKT cells, the percentages of Annexin V-positive cells were slightly decreased from 11.4% to 9.2%, but the mean fluorescence intensities were strikingly diminished from 1493 to 1193 (Figure 7C).

Discussion

The present study confirmed that the expression of AIM was greatly enhanced in macrophages of AIM$^{+/+}$ mice during the stage of *C. parvum*-induced hepatic granuloma formation. AIM deficiency resulted in the enhance-

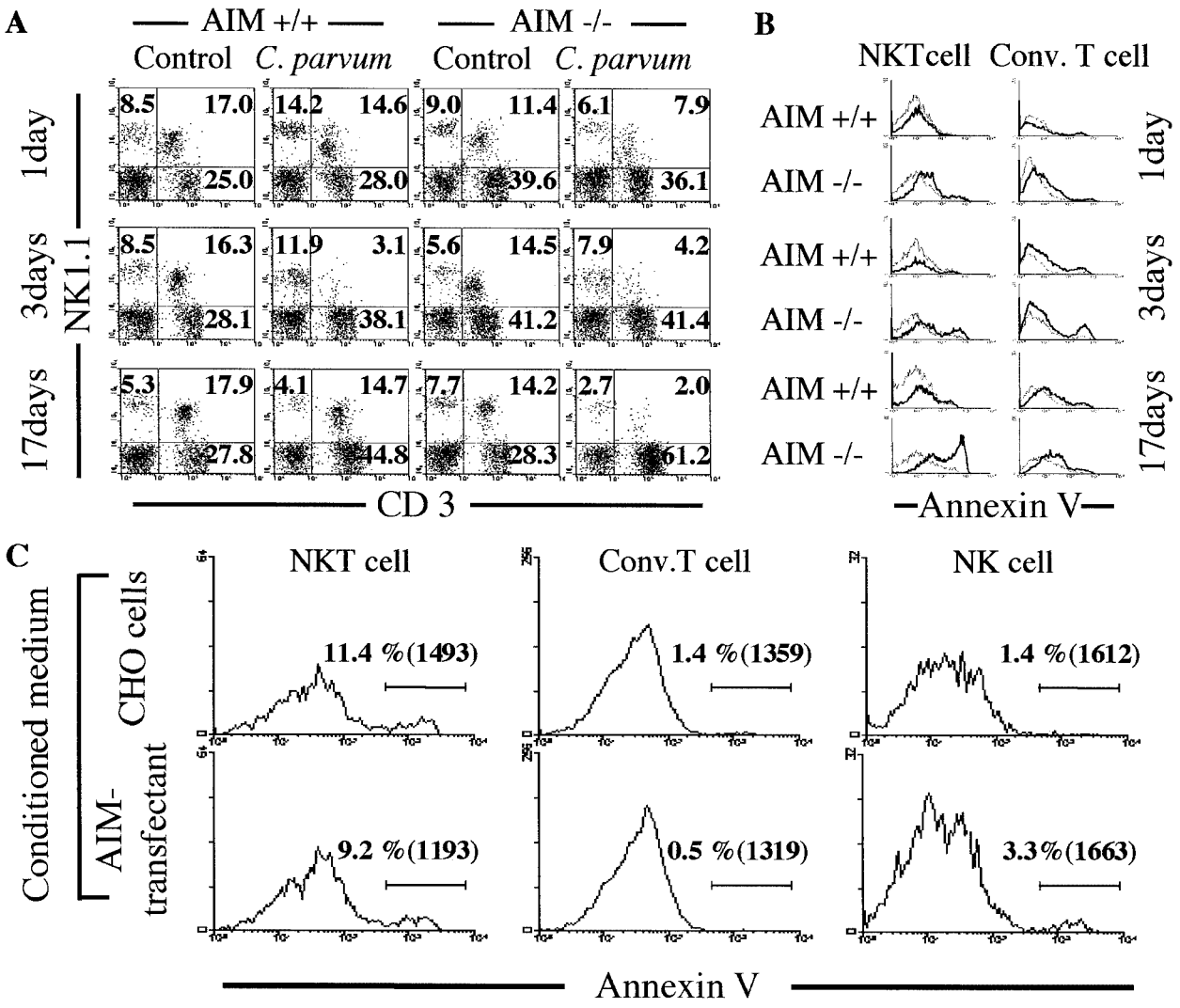

Figure 7. Phenotypic characterization of T cell in the liver of AIM$^{-/-}$ and AIM$^{+/+}$ mice by flow cytometric analysis for CD3 and NK1.1 (**A**) and for CD3, NK1.1, and Annexin V expression (**B**) at 1, 3, and 17 days after *C. parvum* injection. Surface phenotype analysis of cultured cells; liver MNCs (1×10^7 cells per well) were cultured in 24-well microculture plates with (**lower**) or without (**upper**) rAIM protein for 24 hours (**C**). **A:** Proportion of NKT cells were decreased in both mice after *C. parvum* injection. However, repopulation of NKT cells was not observed in the knockout mice at 17 days. Numbers indicate the percentage of fluorescence-positive cells in the corresponding squares. The **right upper gates** exhibit the population of NKT cells, and the **right lower gates** show these of conventional T cells. Typical results from two experiments are shown. **B:** Apoptotic elimination of hepatic NKT cells and conventional T cells in the liver of AIM$^{-/-}$ was more remarkable than that of AIM$^{+/+}$ mice, especially at 1 day and 17 days after *C. parvum* injection. Annexin V-positive NKT cells and conventional T cells in the liver of both mice after *C. parvum* injection are represented by bold histograms, and Annexin V-positive NKT cells and conventional T cells in the liver of each untreated mice are represented by thin histograms. Annexin V-positive cells are induced apoptosis. **C:** Cultured NKT cells with rAIM protein were more diminished in the number and proportion of apoptotic cells, and a few conventional T cells, but not NK cells. Percentages of labeled cells with Annexin V are shown in the histogram. Mean fluorescence intensities are shown in the brackets.

ment of the number and the size of the granulomas. In AIM$^{-/-}$ mice, significantly larger numbers of NKT and T cells underwent apoptosis in the early stage of granuloma formation and repopulation of NKT cells was delayed in the late stage. Recombinant AIM protein rescued the apoptosis of NKT and T cells *in vitro*. These results suggest that AIM plays an important role in the progression and resolution of granulomatous inflammation in part via NKT- and T cell-mediated mechanisms.

The organization and structural maintenance of granulomas requires communication among granuloma-constituting cells. Granulomas are composed mainly of macrophages and lymphocytes. It is believed that T cells within granulomas are crucial to granuloma formation and close association of CD4$^+$ T cells and macrophages represents the interaction of these two cell populations. Beside T cells, NK cells have been detected in high numbers during the early stages of granuloma formation in mice infected with *S. mansoni*.[32] NKT cells have been also detected in *Mycobacterium tuberculosis*, fungal, and intracellular protozoal infection.[33–35] The reported data suggest that NKT cells play a protective role in granulomatous inflammation.

The above-mentioned immunocompeting cells produce various cytokines and soluble factors and these influence granuloma formation. Among cytokines examined in the present study, IL-12 production in AIM$^{-/-}$ mice was larger than in AIM$^{+/+}$ mice after *C. parvum*

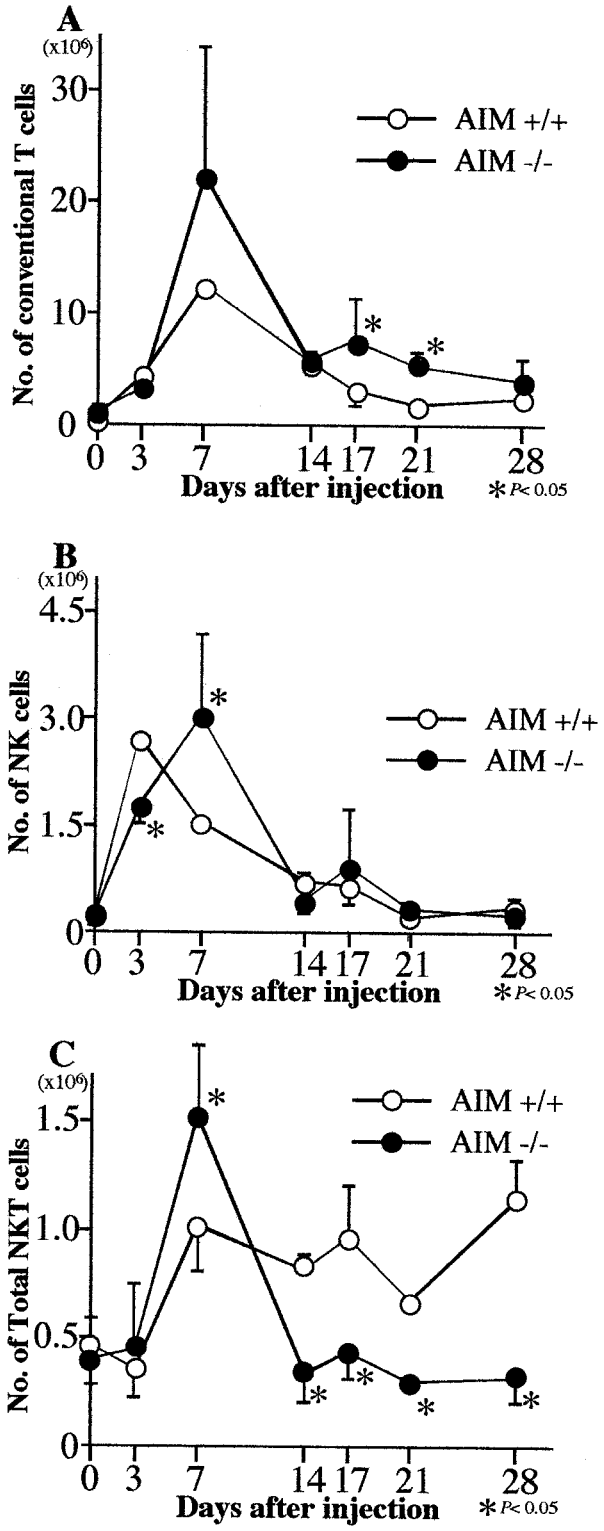

Figure 8. The absolute cell numbers of conventional T cells (**A**), NK cells (**B**), and NKT cells (**C**) in the liver of $AIM^{-/-}$ and $AIM^{+/+}$ mice after *C. parvum* injection. The numbers of NKT cells in the liver of $AIM^{-/-}$ mice became smaller than $AIM^{+/+}$ mice from 14 days after *C. parvum* injection. The absolute cell numbers were calculated on total liver MNCs and the cell subsets obtained from flow cytometric analysis with anti-CD3 and anti-NK1.1 staining. Data are shown as the mean ± SD of three mice. *, $P < 0.05$.

injection in the middle and late stage of granuloma formation. Stimulated antigen-presenting cells such as macrophages or dendritic cells produce IL-12. NKT cells are characterized by prompt production of IL-4 and IFN-γ after IL-12 stimulation and NKT cells have a regulatory function in the IL-12 production by macrophages through the production of IL-4.[36,37] Thus IL-12 has supportive functions for the activation, differentiation, and proliferation of NK and NKT cells.[38,39] The cytokine profiles in the present study indicate that NKT and/or NK cells are closely involved in the *C. parvum*-induced granulomatous inflammation.

In the previous study, we demonstrated enhanced function of macrophages in AIM transgenic mice. More macrophages accumulated in the liver of *C. parvum*- and lipopolysaccharide (LPS)-induced hepatitis of AIM transgenic mice.[11] AIM appears to be associated with hepatitis by supporting macrophage survival at inflammatory sites via apoptosis inhibitory effect, which may contribute to efficient clearance of dead cells and toxic reagents by macrophages. In the present study, phagocytic function of hepatic macrohages in $AIM^{-/-}$ mice was impaired compared to that of $AIM^{+/+}$ mice, indicating that AIM enhance phagocytic function by macrophages. However, granuloma formation was more remarkable in $AIM^{-/-}$ mice than in $AIM^{+/+}$ mice. Because enhanced production of MCP-1 was observed in $AIM^{-/-}$ mice after *C. parvum* injection, it is probable that chemokine production is involved in the function of AIM.

Another interesting finding in the present study was the poor repopulation of NKT cells in the middle and late stages of granuloma formation in $AIM^{-/-}$ mice compared to $AIM^{+/+}$ mice. NKT cells are differentially distributed not only in the liver but also in other tissues such as thymus and spleen, but their physiological or pathological role in the organs remains unclear. NKT cell population expanded after *Malaria*[40–42] and *Leishmania* infection.[43] In contrast, selective depletion of hepatic NKT cells was observed in mice after injection of mycobacterial cord factor, anti-CD3 mAb, IL-12, or α-galactosylceramide, but NKT cells soon repopulate.[33,44,45] In the present study, NKT cells were depleted after *C. parvum* injection. As to the factors inducing NKT cell recruitment, MIP-2 has been recently reported to recruit NKT cells to the spleen during tolerance induction[46] and NKT cells increased in *Cryptococcal* infection in a MCP-1-dependent manner.[35] Further studies are necessary to clarify the regulatory role of AIM in chemokine production for macrophages and NKT cell recruitment.

It is known that NKT cells have great sensitivity to apoptosis.[47,48] We have observed that NKT cells and T cells underwent apoptosis at day 1 after *C. parvum* injection, suggesting that AIM is involved in regulating inflammation progression by preventing apoptosis of NKT cells. Using rAIM, we found a new AIM function as an apoptosis inhibitor to NKT cells *in vitro*. In $AIM^{-/-}$ mice, NKT cells were diminished by a lack of AIM, therefore IL-12 secreted from activated macrophages may stimulate only NK cells. Activated NK cells should secrete IFN-γ, and further re-enhance macrophages by IFN-γ. NK cells are able to promote Th1 differentiation by IFN-γ and NKT

cells modulate the switching from Th0 to Th1, or to Th2, by secreted IFN-γ or IL-4, respectively.[49–51] Low or equal levels of IL-10 and IL-4 expressions in the liver and in the serum of AIM$^{-/-}$ mice, compared to the AIM$^{+/+}$ mice, suggested that switching from Th0 to Th2 was not efficiently accomplished due to the diminished NKT cells. Hence, it seemed reasonable to consider that diminishing NKT cell enhanced Th1 type response in AIM$^{-/-}$ mice. Higher IFN-γ mRNA expression in the liver and higher IFN-γ serum concentration in AIM$^{-/-}$ mice may support this assumption.

In summary, AIM produced by macrophages is involved in *C. parvum*-induced granuloma formation. Enhanced and prolonged granuloma formation in AIM$^{-/-}$ mice indicate that AIM plays an important role in host defense mechanisms against inflammation in the initial and healing stage. It was also suggested that AIM regulates NKT cell and T cell apoptosis and recruitment.

References

1. Miyazaki T, Hirokami Y, Matsuhashi N, Takatsuka H, Naito M: Increased susceptibility of thymocytes to apoptosis in mice lacking AIM, a novel murine macrophage-derived soluble factor belonging to the scavenger receptor cysteine-rich domain superfamily. J Exp Med 1999, 189:413–422
2. Oyama H, Yamada T, Inoue Y: Effect of post-irradiation temperature on viability of rat thymocytes. Int J Radiat Biol Relat Stud Phys Chem Med 1974, 26:535–546
3. Ohyama H, Yamada T, Ohkawa A, Watanabe I: Radiation-induced formation of apoptotic bodies in rat thymus. Radiat Res 1985, 101: 123–130
4. Bodey B, Bodey Jr B, Kaiser HE: Apoptosis in the mammalian thymus during normal histogenesis and under various in vitro and in vivo experimental conditions. In Vivo 1998, 12:123–133
5. Selye H: Thymus and adrenals in the response of the organism to injuries and intoxication. Br J Exp Pathol 1936, 17:234–248
6. Dougherty TF: Effect of hormones on lymphatic tissue. Physiol Rev 1952, 32:379–401
7. Wyllie AH: Glucocorticoid-induced thymocyte apoptosis is associated with endogenous endonuclease activation. Nature 1980, 284: 555–556
8. Cohen JJ: Glucocorticoid-induced apoptosis in the thymus. Semin Immunol 1992, 4:363–369
9. Gruber J, Sgonc R, Hu YH, Beug H, Wick G: Thymocyte apoptosis induced by elevated endogenous corticosterone levels. Eur J Immunol 1994, 24:1115–1121
10. Yusa S, Ohnishi S, Onodera T, Miyazaki T: AIM, a murine apoptosis inhibitory factor, induces strong and sustained growth inhibition of B lymphocytes in combination with TGF-β 1. Eur J Immunol 1999, 29:1086–1093
11. Haruta I, Kato Y, Hashimoto E, Minjares C, Kennedy S, Uto H, Yamauchi K, Kobayashi M, Yusa S, Muller U, Hayashi N, Miyazaki T: Association of AIM, a novel apoptosis inhibitory factor, with hepatitis via supporting macrophage survival and enhancing phagocytotic function of macrophages. J Biol Chem 2001, 276:22910–22914
12. Adams DO: The biology of the granuloma. Pathology of Granulomas. Edited by HL Ioachim. New York, Raven Press, 1983, pp 1–20
13. Adams DO, Hamilton TA: Macrophages as destructive cells in host. Inflammation: Basic Principles and Clinical Correlates, ed 2. Edited by JI Gallin, IM Goldstein, R Snyderman. New York, Raven Press, 1992, pp 637–662
14. Cory S: Regulation of lymphocyte survival by the bcl-2 gene family. Annu Rev Immunol 1995, 13:513–543
15. Chao DT, Korsmeyer SJ: BCL-2 family: regulators of cell death. Annu Rev Immunol 1998, 16:395–419
16. Steller H: Mechanisms and genes of cellular suicide. Science 1995, 267:1445–1149
17. Thompson CB: Apoptosis in the pathogenesis and treatment of disease. Science 1995, 267:1456–1462
18. Jacobson MD, Weil M, Raff MC: Programmed cell death in animal development. Cell 1997, 88:347–354
19. Vaux DL, Haecker G, Strasser A: An evolutionary perspective on apoptosis. Cell 1994, 76:777–779
20. Raff MC: Social controls on cell survival and cell death. Nature 1992, 356:397–400
21. Yang E, Korsmeyer SJ: Molecular thanatopsis: a discourse on the BCL2 family and cell death. Blood 1996, 88:386–401
22. Strasser A, Huang DC, Vaux DL: The role of the bcl-2/ced-9 gene family in cancer and general implications of defects in cell death control for tumourigenesis and resistance to chemotherapy. Biochim Biophys Acta 1997, 1333:F151–F178
23. Yamada M, Naito M, Takahashi K: Kupffer cell proliferation and glucan-induced granuloma formation in mice depleted of blood monocytes by strontium-89. J Leukocyte Biol 1990, 47:195–205
24. Naito M, Takahashi K: The role of Kupffer cells in glucan-induced granuloma formation in the mouse liver depleted of blood monocytes by administration of strontium-89. Lab Invest 1991, 50:664–674
25. Takahashi K, Naito M, Umeda S, Shultz LD: The role of macrophage colony-stimulating factor in hepatic glucan-induced granuloma formation in the osteopetrosis mutant mouse defective in the production of macrophage colony-stimulating factor. Am J Pathol 1994, 144: 1381–1392
26. Moloney W, McPherson K, Fliegelman L: Esterase activity in leukocytes demonstrated by the use of naphthol AS-D chloroacetate substrate. J Histochem Cytochem 1960, 8:200–207
27. Isobe S, Nakane PK, Brown WR: Studies on translocation of immunoglobulins across intestinal ephithelium. 1. Improvements to study the peroxidase-labeled antibody method for application to study of human intestinal mucosa. J Histochem Cytochem 1977, 10:167–171
28. Austyn JM, Gordon S: F4/80, a monoclonal antibody directed specifically against the mouse macrophage. Eur J Immunol 1981, 11:805–815
29. Gabirieli Y, Sherman Y, Ben-Sasson AS: Identification of programmed cell death in situ via specific labeling of nuclear DNA fragmentation. J Cell Biol 1992, 119:493–501
30. Watanabe H, Miyaji C, Seki S, Abo T: c-kit^{+} stem cells and thymocyte precursors in the liver of adult mice. J Exp Med 1996, 184:687–693
31. Vermes I, Haanen C, Steffens-Nakken H, Reutelingsperger C: A novel assay for apoptosis: flow cytometric detection of phosphatidylserine expression on early apoptotic cells using fluorescein labelled Annexin V. J Immunol Methods 1995, 184:39–51
32. Remick DG, Chensue SW, Hiserodt JC, Higashi GI, Kunkel SL: Flow-cytometric evaluation of lymphocyte subpopulations in synchronously developing Schistosoma mansoni egg and Sephadex bead pulmonary granulomas. Am J Pathol 1988, 131:298–307
33. Apostolou I, Takahama Y, Belmant C, Kawano T, Huerre M, Marchal G, Cui J, Taniguchi M, Nakauchi H, Fournie J-J, Kourilsky P, Gachelin G: Murine natural killer cells contribute to the granulomatous reaction caused by mycobacterial cell walls. Proc Natl Acad Sci USA 1999, 96:5141–5146
34. Kawakami K, Kinjo Y, Yara S, Koguchi Y, Uezu K, Nakayama T, Taniguchi M, Saito A: Activation of Vα14^{+} natural killer T cells by α-galactosylceramide results in development of Th1 response and local host resistance in mice infected with Cryptococcus neoformans. Infect Immun 2001, 69:213–220
35. Kawakami K, Kinjo Y, Uezu K, Yara S, Miyagi K, Koguchi Y, Nakayama T, Taniguchi M, Saito A, Saito A: Monocyte chemoattractant protein-1-dependent increase of Vα14^{+} NKT cells in lungs and their roles in Th1 response and host defense in Cryptococccal infection. J Immunol 2001, 167:6525–6532
36. Naiki Y, Nishimura H, Kwano T, Tanaka Y, Itohara S, Taniguchi M, Yoshikai Y: Regulatory role of peritoneal NK1.1$^{+}\alpha\beta$ cells in IL-12 production during Salmonella infection. J Immunol 1999, 163:2057–2063
37. Joyce S, Woods AS, Yewdell JW, Bennink JR, De Silva AD, Boesteanu A, Balk SP, Cotter RJ, Brutkiewicz RR: Natural ligand of mouse CD1d1: cellular glycosylphosphatidylinositol. Science 1998, 279:1541–1544
38. Gately MK, Desai BB, Wolitzky AG, Quinn PM, Dwyer CM, Podlaski FJ, Familletti PC, Sinigaglia F, Chizonnite R, Gubler U, Stern AS: Regulation of human lymphocyte proliferation by a heterodimeric

cytokine, IL-12 (cytotoxic lymphocyte maturation factor). J Immunol 1991, 147:874–882
39. Todt JC, Whitfield JR, Ivard SR, Boros DL: Down-regulation of interleukin-12, interleukin-12R expression/activity mediates the switch from Th1 to Th2 granuloma response during murine Schistosomiasis mansoni. Scand J Immunol 2000, 52:385–392
40. Gonzalez-Aseguinolaza G, de Oliveira C, Tomaska M, Hong S, Bruna-Romero O, Nakayama T, Taniguchi M, Bendelac A, Van Kaer L, Koezuka Y, Tsuji M: α-galactosylceramide-activated Vα14 natural killer T cells mediate protection against murine malaria. Proc Natl Acad Sci USA 2000, 97:8461–8466
41. Weerasinghe A, Sekikawa H, Watanabe H, Mannoor MK, Morshed SRM, Halder RC, Kawamura T, Kosaka T, Miyaji C, Kawamura H, Seki S, Abo T: Association of intermediate T cell receptor cells, mainly their NK1.1^{-} subset, with protection from malaria. Cell Immunol 2001, 207:28–35
42. Kaiissar Mannoor M, Weerasinghe A, Halder RC, Reza S, Morshed M, Ariyasinghe A, Watanabe H, Sekikawa H, Abo T: Pesistance to malarial infections achieved by the cooperation of NK1.1^{+} and NK1.1^{-} subsets of intermediate TCR cells which are constituents of innate immunity. Cell Immunol 2001, 211:96–104
43. Ishikawa H, Hisaeda H, Taniguchi M, Nakayama T, Sakai T, Maekawa Y, Nakano Y, Zhang M, Zhang T, Nishitani M, Takashima M, Himeno K: CD4^{+} Vα14 NKT cells play a crucial role in an early stage of protective immunity against infection with Leishmania major. Int Immunol 2000, 12:1267–1274
44. Eberl G, MacDonald HR: Rapid death and regeneration of NKT cells in anti-CD3ε- or IL-12-treated mice: a major role for bone marrow in NKT cell homeostasis. Immunity 1998, 9:345–353
45. Nakagawa R, Nagafune I, Tazunoki Y, Ehara H, Tomura H, Iijima R, Motoki K, Kamishohara M, Seki S: Mechanisms of the antimetastatic effect in the liver and of the hepatocyte injury by α-galactosylceramide in mice. J Immnol 2001, 166:6578–6584
46. Faunce DE, Sonoda KH, Streilein J: MIP-2 recruits NKT cells to the spleen during tolerance induction. J Immunol 2001, 166:313–321
47. Leite-de-Moraes MC, Herbelin A, Gouarin C, Koezuka Y, Schneider E, Dy M: Fas/Fas ligand interactions promote activation-induced cell death of NK T lymphocytes. J Immunol 2000, 165:4367–4371
48. Osman Y, Kawamura T, Naito T, Takeda K, Van Kaer L, Okumura K, Abo T: Activation of hepatic NKT cells and subsequent liver injury following administration of α-galactosylceramide. Eur J Immunol 2000, 30:1919–1928
49. Arase H, Arase N, Nakagawa K, Good RA, Onoe K: NK1.1^{+} CD4^{+} CD8^{-} thymocytes with specific lymphokine secretion. Eur J Immunol 1993, 23:307–310
50. Singh N, Hong S, Scherer DC, Serizawa I, Burdin N, Kronenberg M, Koezuka Y, Van Kaer L: Cutting edge: activation of NK T cells by CD1d and α-galactosylceramide directs conventional T cells to the acquisition of a Th2 phenotype. J Immunol 1999, 163:2373–2377
51. Bendelac A, Hunziker RD, Lantz O: Increased interleukin 4 and immunoglobulin E production in transgenic mice overexpressing NK1 T cells. J Exp Med 1996, 184:1285–1293